The MC events were first passed through the candidate selection procedure. Then the average deviation $(x_{\rm MC} - x_{\rm REC})$ and the r.m.s.(root mean square) of the deviation were calculated for each $x_{\rm REC}$ bin(iterated twice to get rid of long tails). The deviations are shown in Figure 40 and Figure 41. The r.m.s. of the deviations are shown as the vertical error bars.

7.4 Comparison of the data and Monte Carlo simulation

In this analysis, acceptance correction is based on the average acceptance $\langle\epsilon\rangle$ defined by

$$\langle\epsilon\rangle = \frac{\int \epsilon d\sigma_{ep}}{\int d\sigma_{ep}} \tag{69}$$

If the Monte Carlo generator reproduces the true distributions correctly, then the average acceptance can be determined simply by counting number of generated events and number of selected events. Figure 42 to Figure 46 show the comparisons of the J/ψ candidates and four Monte Carlo simulations in p_t^2 of J/ψ, $y_{\rm rap}$, $\sqrt{s_{\gamma p}}$, $\theta_{J/\psi}$ and the decay cosine($\cos\theta_{\rm decay}$). Figure 49 to Figure 53 show the acceptance in these variables. Perhaps none of the MC agree with the real data in all regions of all variables. Apart from revealing disagreement between the true $d\sigma_{ep}/dx$ and $d\sigma_{ep}^{(MC)}/dx$ of the models, some errors in detector simulation of $\epsilon(x)$ may also be observable in these figures(x stands for one or a set of kinematic variables). For example, the angular distribution of e^+ and e^- should agree in any model and in the real data. However, Figure 47 and Figure 48 may indicate disagreement(it may or may not be accounted for by statistical fluctuations) in the real data between $\cos\theta_{e^+}$ and $\cos\theta_{e^-}$(in the laboratory frame). The two peak structure of the decay angular distribution in the real data (Figure 46) is not expected from any model. The disagreement between the real data and the MC in $\cos\theta_{\rm decay}$ perhaps reveals error in $\epsilon(x)$. It may also be due to statistical fluctuations and effects of pion contamination. The steep peak in $y_{\rm rap}$ of the real data may also be due to either pion contamination or systematic effects on $\epsilon(x)$.

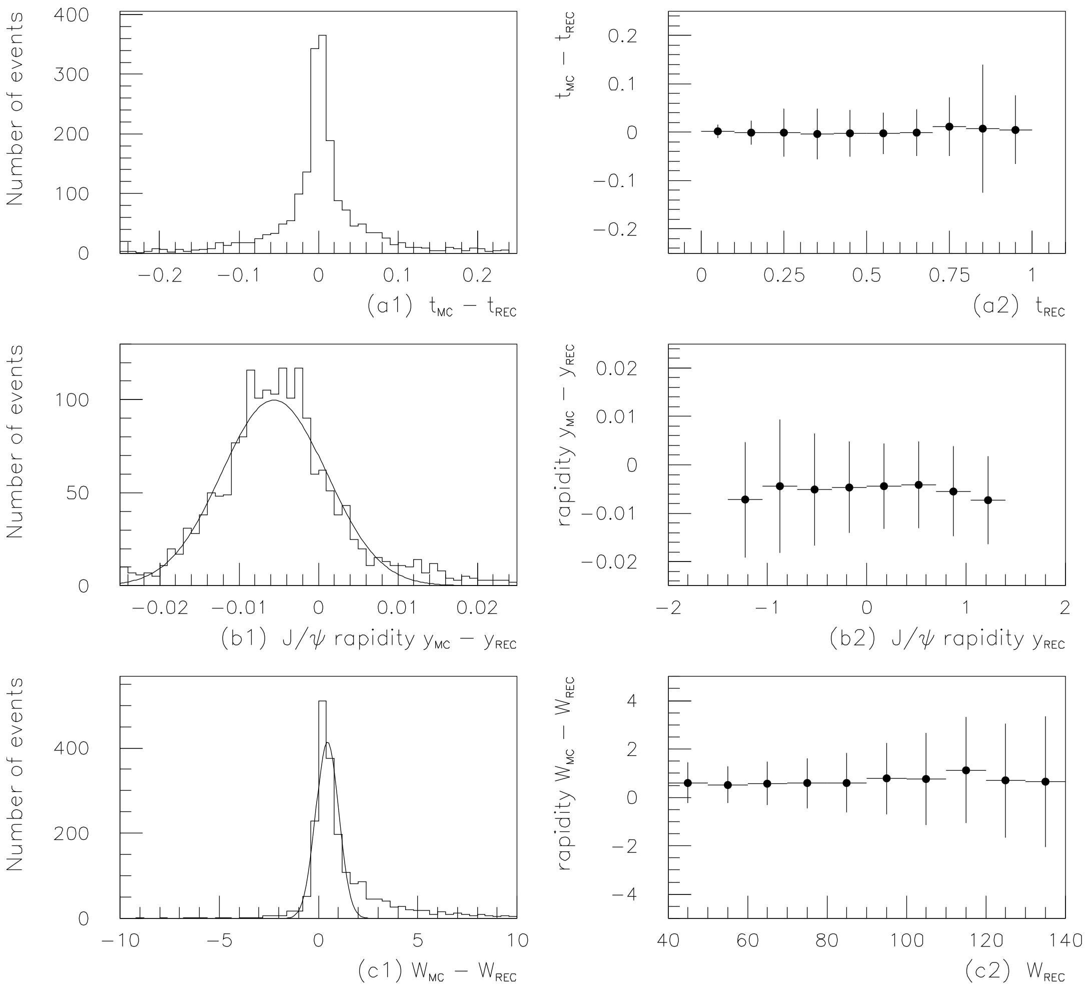

Figure 40: Resolution of reconstructed J/ψ kinematic variables. Monte Carlo elastic $J/\psi \to e^+e^-$ events passing the trigger and selection cuts were used. Left(a1,b1,c1): histograms of the difference between the reconstructed and generated values. Right(a2,b2,c2): bin average difference between reconstructed and generated values for each bin. The vertical error bars represent the r.m.s. of the difference. (a): resolution of p_t^2 of J/ψ. (b): resolution of y_{rap}(true rapidity of J/ψ). (c): resolution of track p_t of electrons.

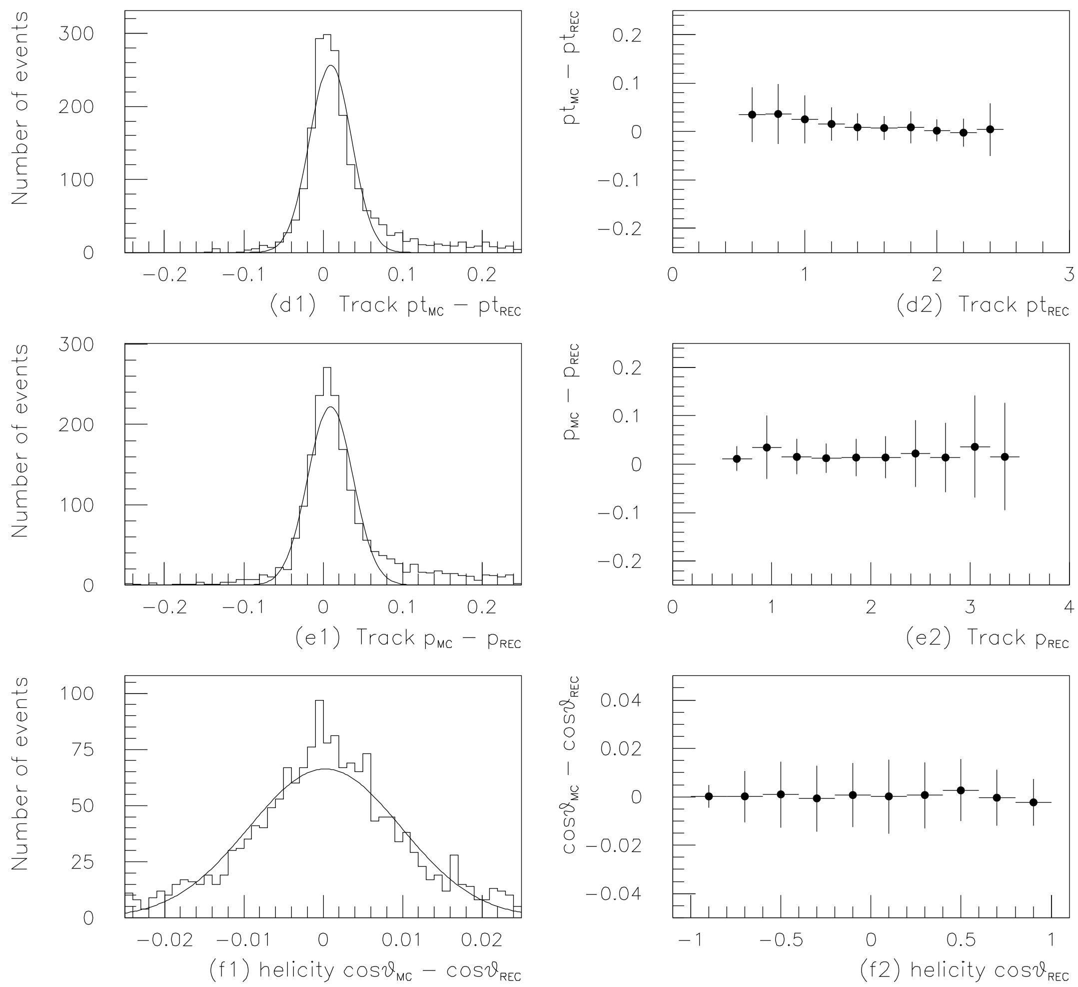

Figure 41: Resolution of reconstructed track variables. Monte Carlo elastic $J/\psi \to e^+e^-$ events passing the trigger and selection cuts were used. Left(d1,e1,f1): histograms of the difference between the reconstructed and generated values. Right(d2,e2,f2): bin average difference between reconstructed and generated values for each bin. The vertical error bars represent the r.m.s. of the difference. (d): resolution of track p_t. (e): resolution of track p. (f): resolution of $\cos\theta_{decay}$.

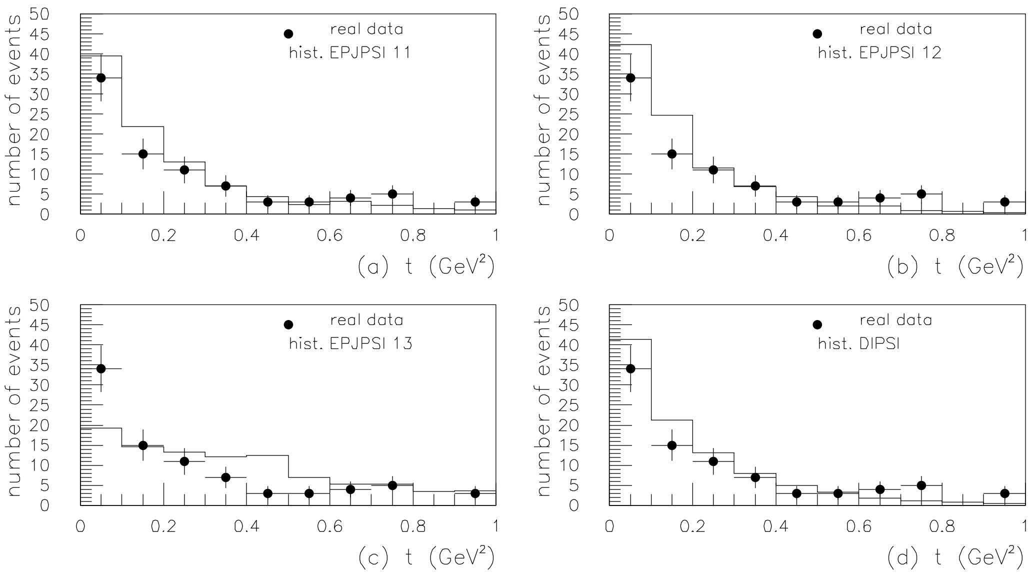

Figure 42: Comparison of t dependence.

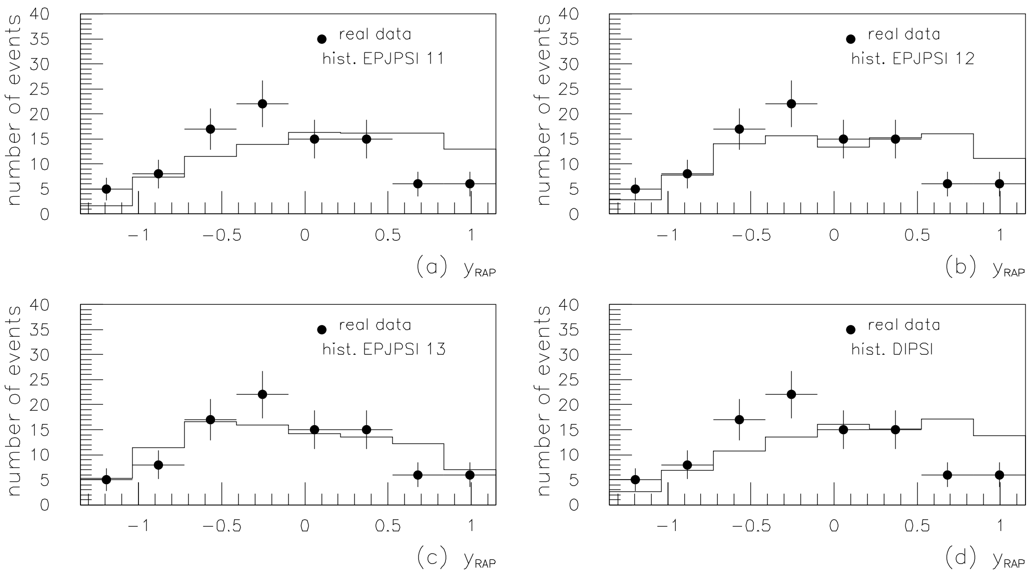

Figure 43: Comparison of $y_{\rm rap}$ distribution.

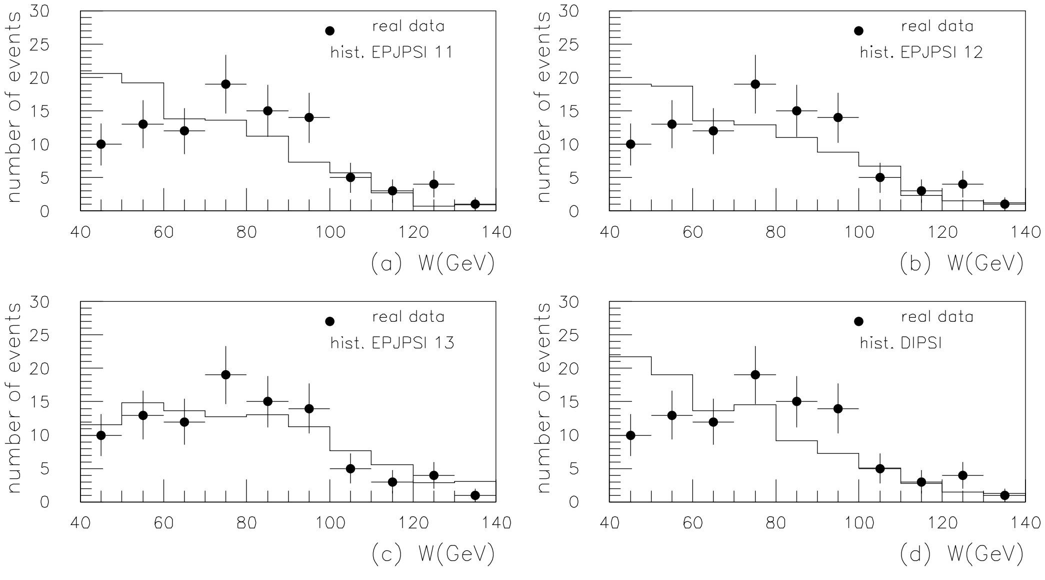

Figure 44: Comparison of $\sqrt{s_{\gamma p}}$ distribution.

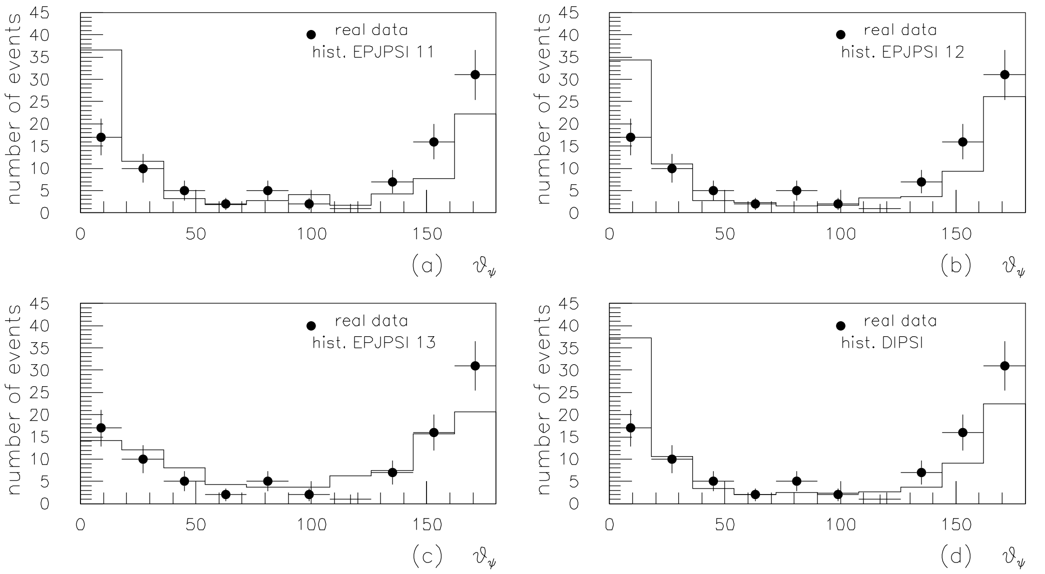

Figure 45: Comparison of θ of J/ψ distribution.

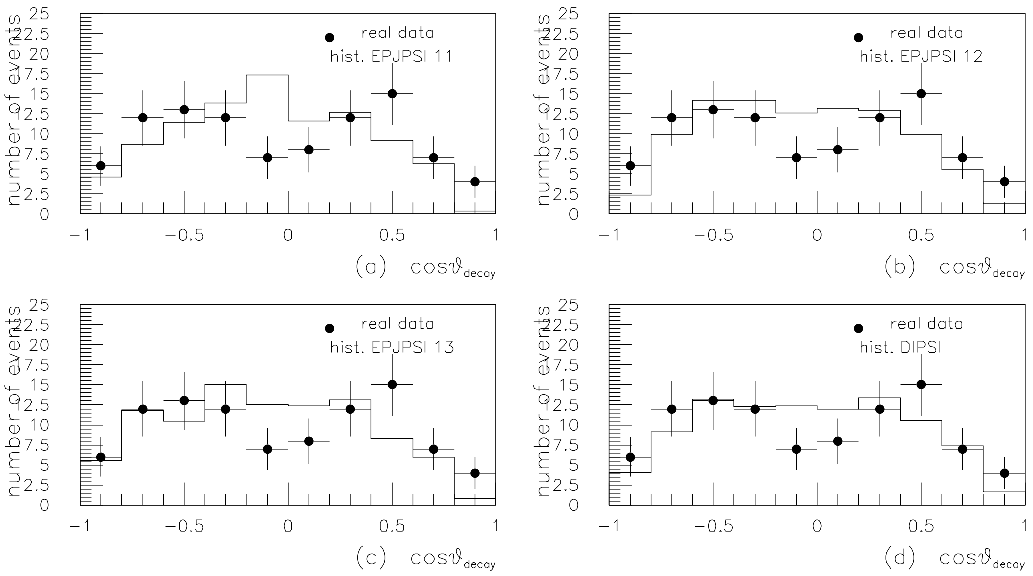

Figure 46: Comparison of the decay cosine distribution.

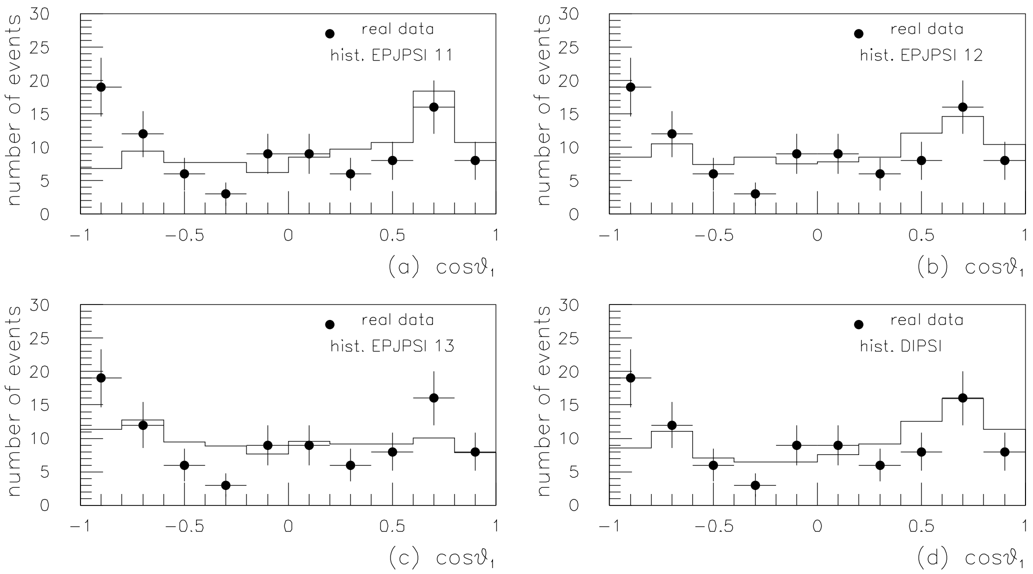

Figure 47: Comparison of the e^+ cosine distribution.

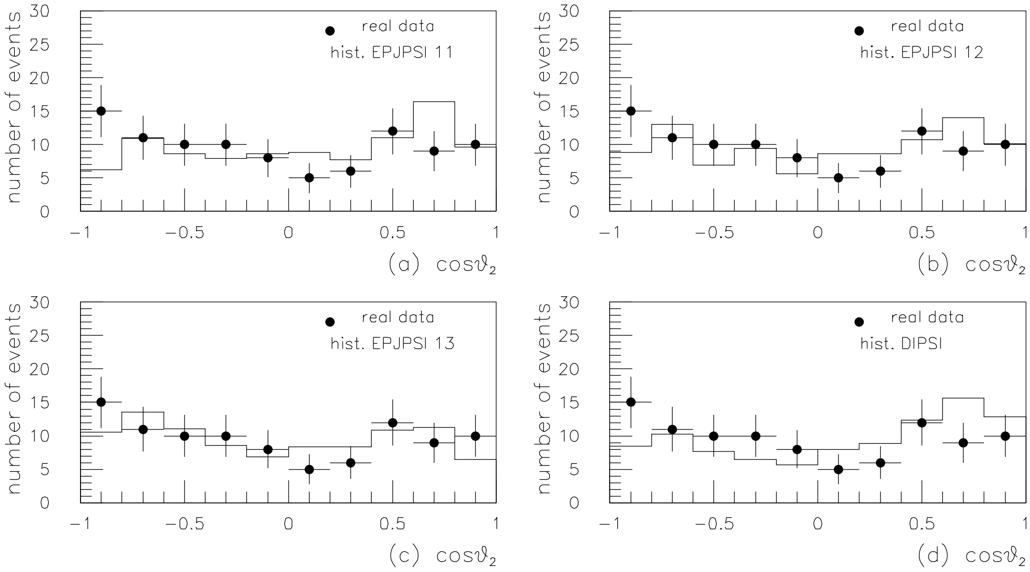

Figure 48: Comparison of e^- cosine distribution.

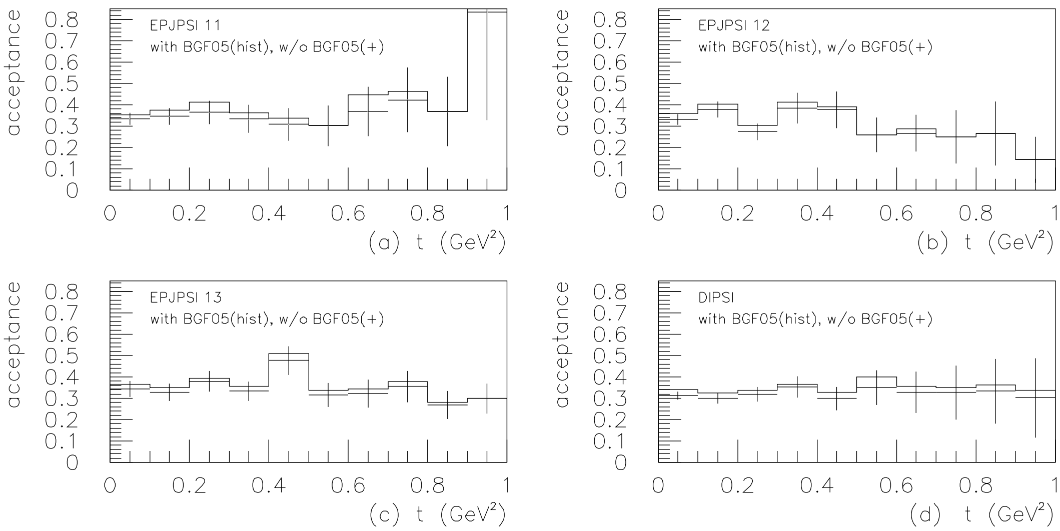

Figure 49: Acceptance as a function of t.

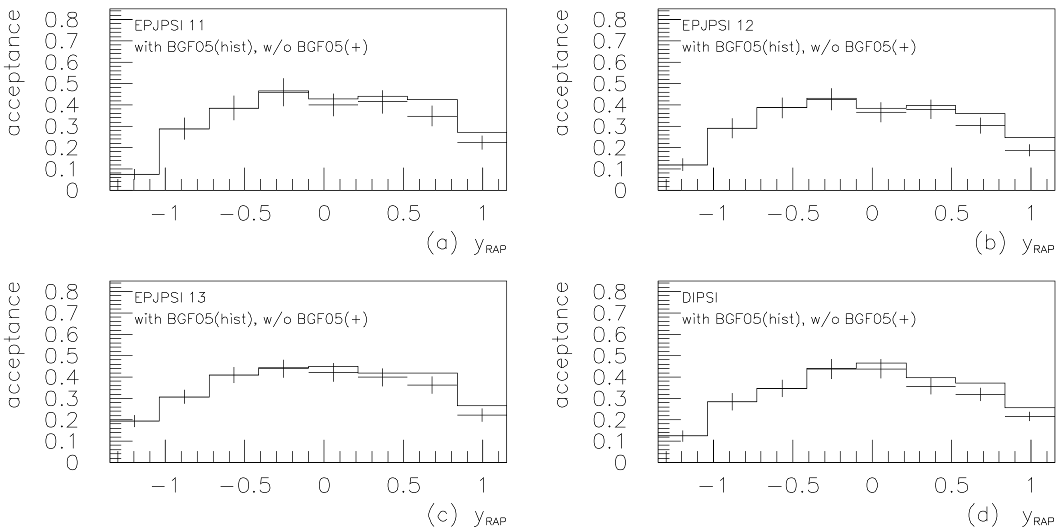

Figure 50: Acceptance as a function of y_{rap}.

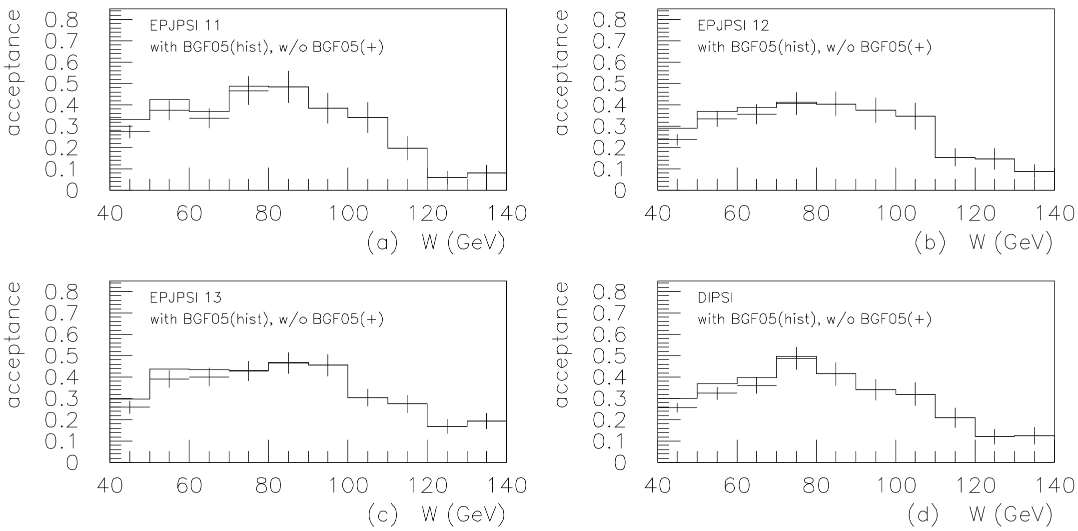

Figure 51: Acceptance as a function of $\sqrt{s_{\gamma p}}$.

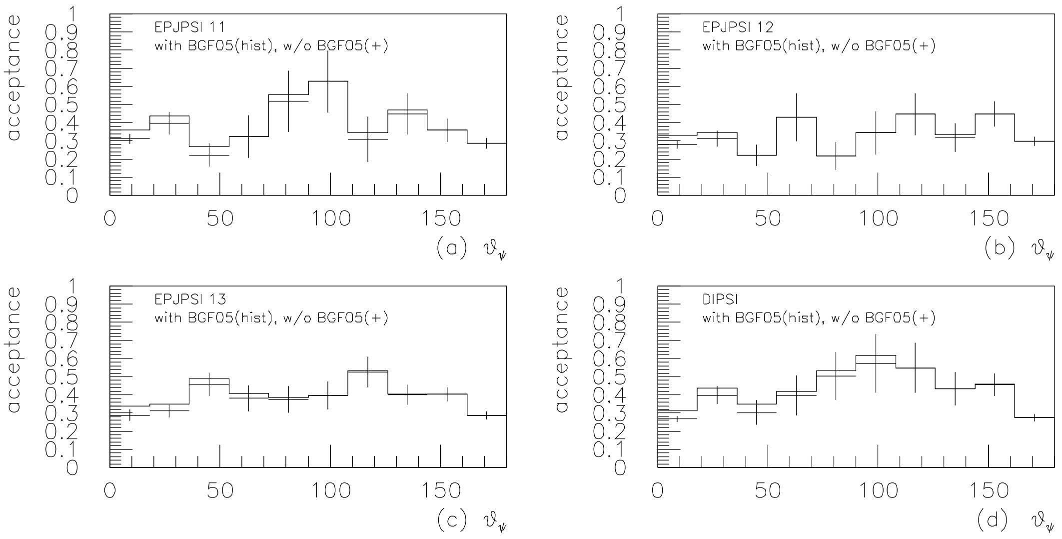

Figure 52: Acceptance as a function of $\theta_{J/\psi}$.

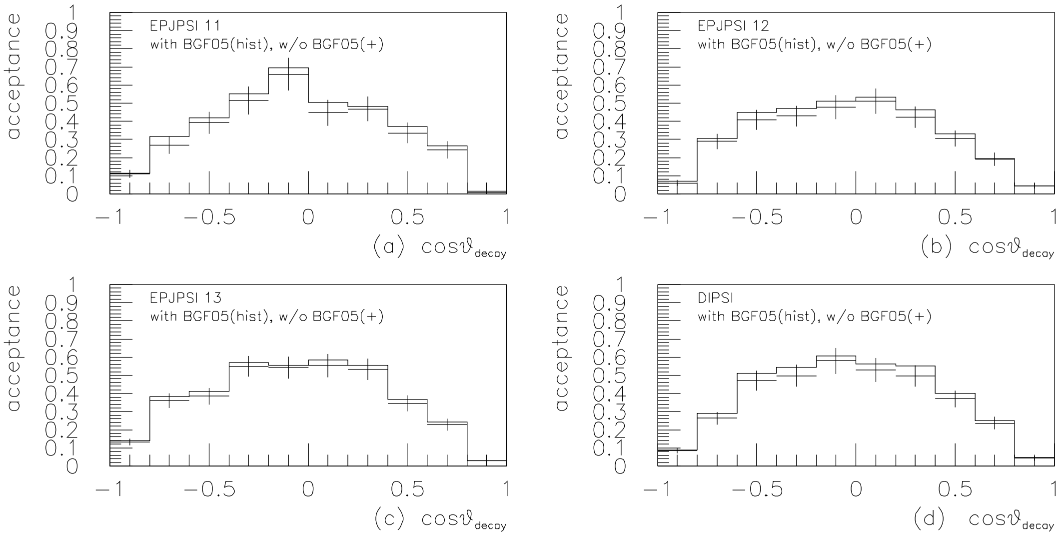

Figure 53: Acceptance as a function of decay cosine.